Jurnal Polimesin
Department of Mechanical Engineering
State Polytechnic of Lhokseumawe
http://e-jurnal.pnl.ac.id/polimesin

e-ISSN	: 2549-1999	No.	: 5	Month	: October
p-ISSN	: 1693-5462	Volume	: 23	Year	: 2025

Processing dates: received on 2025-07-20, reviewed on 2025-08-05, accepted on 2025-08-11 and online availability on 2025-10-31

Dynamic braking performance of a low-mass prototype vehicle under different speeds and loads

Budi Istana*, Abrar Ridwan, Izzazul Kafitra Sitompul
Department of Mechanical Engineering, University of Muhammadiyah Riau, Pekanbaru 28292, Indonesia
*Corresponding Author: budiistana@umri.ac.id

Abstract

Dynamic braking performance is well understood in conventional vehicles, but its characteristics in ultra-lightweight, energy-efficient prototype vehicles remain poorly documented, despite their growing role in energy efficiency competitions and urban mobility concepts. This study experimentally investigated stop braking performance under varying vehicle speeds and masses in a low-mass prototype vehicle (V1.0). Tests were conducted at four speed levels (10, 20, 30, and 40 km/h) and two mass configurations (135 kg and 165 kg), with each scenario repeated five times on a flat 100 m track. With an increase in speed from 30 to 40 km/h, the 135-kg configuration showed increases in braking distance of 11.14 m (133%), braking time of 1.92 s (47%), and disc pad temperature of 0.66 °C (1.5%). The 165-kg configuration showed corresponding increases of 14.21 m (152%), 3.02 s (75%), and 1.40 °C (3.3%). Across the full test range, increasing speed from 10 km/h to 40 km/h for the 135-kg configuration increased braking distance from 1.78 m to 19.5 m (+995%) and braking time from 1.63 s to 5.04 s (+209%). Increasing mass from 135 kg to 165 kg at 30 km/h increased braking distance by 0.97 m (11.6%) and braking time by 0.59 s (17.3%). Disc pad temperatures remained within a safe range, rising only from 41.1 °C to 42.5 °C (+3.4%) across the tested speeds. These quantitative findings provide critical data for optimizing braking system design in lightweight, energy-efficient prototypes, ensuring operational safety under various load and speed conditions.

Keywords:
Braking distance, braking time, disc pad temperature, vehicle dynamics, and vehicle mass

1 Introduction

The Energy-Efficient Car Competition (EECC) is a prestigious annual event that encourages university students to design and develop prototype vehicles focused on energy efficiency. In this competition, efficiency is the primary benchmark. However, safety aspects such as the braking system are also crucial in determining the overall feasibility and performance of the vehicle. EECC prototype vehicles are generally lightweight, have aerodynamic shapes, and utilize simplified mechanical systems to minimize energy consumption. These conditions, however, require careful attention in designing the braking system to ensure adequate vehicle control and safety.

Braking is a critical process in the vehicle control system that directly relates to driver safety. When the vehicle is moving and braking is applied, the frictional force generated by the brake system functions to reduce the vehicle's kinetic energy until it reaches a complete stop. This process is influenced by various factors, including initial speed, total vehicle weight, road surface conditions, and the type of braking system used. According to Gillespie [1] and Wong [5], braking dynamics are highly dependent on the interaction between the braking system, mass distribution, and wheel condition, all of which must be balanced to maintain stability during deceleration.

Vehicle speed has a significant effect on braking distance. The higher the initial speed, the greater the kinetic energy that must be dissipated as heat through the braking system. Kinetic energy is directly proportional to the mass of the vehicle and increases with the square of the velocity. Therefore, an increase in speed causes an exponential increase in braking distance. A study by Chen et al [6], and by Chen, Chiu, and Hsiau [7] revealed that in lightweight vehicles, increasing the speed from 20 km/h to 40 km/h could extend the braking distance by up to 150%, depending on road conditions and braking system types.

In addition to speed, vehicle weight also contributes to braking performance. A heavier vehicle has greater momentum, which requires more braking force to bring the vehicle to a stop [8]. For lightweight vehicles such as EECC prototypes, changes in mass due to payload or structural design variations can significantly affect braking behavior. Berjoza et al, found that in vehicles weighing less than 200 kg, a 20% increase in weight could result in a 12% longer braking distance, depending on load distribution and brake type [9].

Several previous studies have discussed braking in the context of conventional or electric vehicles, but specific research on ultra-lightweight vehicles like EECC prototypes remains limited. Moreover, most studies tend to focus on brake system development rather than on the influence of physical vehicle parameters [4], [10]. Liu *et al.* highlighted the need for further studies on low-mass vehicles to better understand how braking dynamics behave under maximum energy efficiency conditions [11].

This study focuses specifically on stop braking, in which the prototype vehicle is decelerated from a given initial speed to a complete stop, enabling measurement of braking distance, braking time, and disc pad temperature under different mass and speed configurations.

2 Research methodology

The object of the study was the V1.0 prototype car, as shown in Fig. 1. The braking tests were conducted on a 100 m flat asphalt track under dry conditions. The vehicle was accelerated to the target test speed (10, 20, 30, or 40 km/h) and maintained until reaching a marked brake initiation point.

Fig. 1. V1.0 prototype car

At this marker, the driver applied maximum brake force to bring the vehicle to a complete stop. Braking distance was measured from the brake initiation point to the stop line using a calibrated measuring tape, while braking time was recorded from the instant of pedal application until the vehicle stopped, using a Seiko® S23601P stopwatch. Immediately after each stop, disc pad temperature was recorded using a Sanfix IT-550N infrared thermometer. Each speed–mass configuration was tested five times, with a minimum three-minute cooling interval between runs to avoid heat build-up. Figs. 2 and 3 illustrate the braking system configuration and the experimental track layout, respectively, providing visual documentation of the test setup and procedure.

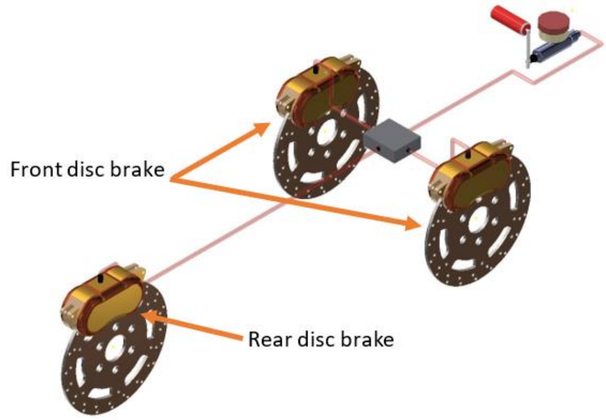

Fig. 2. Schematic system hydraulic disc brake of the V1.0 prototype car

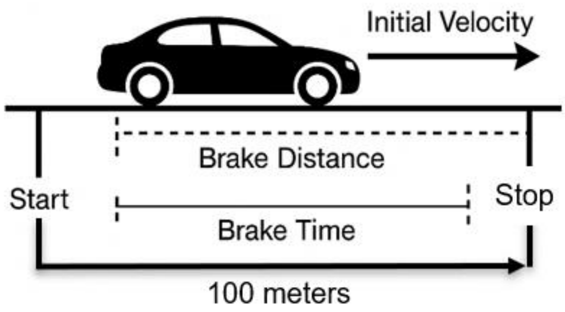

Fig. 3. Experimental Scenario – Braking was initiated at the designated point and measured until the vehicle came to a complete Stop

The tested prototype V1.0 is a three-wheeled, ultra-lightweight vehicle with a tubular steel frame, aerodynamic fiberglass body, and hydraulic disc brakes on both front and rear wheels. The unloaded vehicle mass is 85 kg, and with driver configurations of 50 kg and 80 kg, the total test masses were 135 kg and 165 kg, as detailed in Table 1.

Table 1. Summary of experimental variables and measurement parameters for stop braking tests

Aspect	Description
Independent variables	• Vehicle initial speed: 20 km/h, 30 km/h, 40 km/h • Vehicle weight: 135 kg, 165 kg
Dependent variables	• Braking distance (m) • Braking time (s) • Brake pad temperature (˚C)
Controlled variables	• Tire pressure: standardized to 40 psi • Vehicle weight: 85 kg • Driver weight 1: 50 kg • Driver weight 2: 80 kg • Road surface: dry and clean asphalt
Measurement tools	• Digital Laser RPM Tacho Meter DT2234C • Stopwatch Seiko S23601P • Measuring tape (30 m) • Sanfix IT-550N Digital Infrared Laser Thermometer • Digital weighing scale
Data collection method	• The prototype was accelerated to the target speed (10, 20, 30, or 40 km/h) • Braking was initiated at a fixed test point • Braking distance was measured from the braking point until the vehicle stopped completely • Braking time was recorded from pedal actuation to stop • Disc pad temperatures were measured immediately after each test • Tests were repeated five times for each condition to calculate the average and standard deviation
Data analysis	Data analysis was carried out in Python, calculating means and standard deviations, and plotting graphs with error bars to visualize variability and repeatability

The braking system is mechanically balanced, with hydraulic lines providing equal brake fluid pressure to both front and rear calipers. Under dynamic braking, weight transfer causes approximately 60% of the braking force to act on the front wheels and 40% on the rear wheels at the start of deceleration.

The methods for calculating kinetic energy and deceleration were based on classical mechanics, drawing on established formulations as presented [1]. These references provide the foundational equations used in vehicle dynamics analysis and braking force evaluation. The theoretical basis ensures that the derived results are consistent with accepted engineering principles and applicable to prototype vehicle performance studies. To enhance the analysis of braking behavior, two physical quantities were calculated and illustrated in equation form. Kinetic energy (E_k) was calculated to quantify the mechanical energy that the braking system must dissipate during each trial. The formula used is Eq. (1).

$$E_k = \frac{1}{2}mv^2 \tag{1}$$

where E_k is kinetic energy in Joules (J), m is the mass of the vehicle (kg), and v is velocity in meters per second (m/s). This computation reflects the energy reserve associated with motion, which grows quadratically with velocity, highlighting how even small speed increases produce large increases in energy demands.

The estimated deceleration (a) is approximated by assuming uniform deceleration from the initial velocity to a complete stop, so that the formula applied is Eq. (2), where a is deceleration (m/s²), and t is braking time (s), measured from brake application to complete stop.

$$a = \frac{v}{t} \tag{2}$$

These derived parameters provide critical insight into the energy absorption and braking effectiveness under varying mass-speed conditions, especially in prototype vehicles with minimal braking systems.

3 Results and discussion

Table 2 summarizes the key findings from the experimental braking tests for both vehicle masses across all tested speeds. It includes average and standard deviation values for braking distance, braking time, disc pad temperature, as well as the calculated kinetic energy and estimated deceleration.

Table 2. Summary of experimental braking tests

Vehicle mass (kg)	Speed (km/h)	Brake distance (m)		Brake time (s)		Brake pad temp (°C)		Kinetic energy (J)	Deceleration (m/s^2)
135	10	1.78	±0.13	1.63	±0.542	41.13	±1.15	521.67	1.89
135	20	6.86	±1.14	3.22	±0.439	41.40	±0.89	2086.67	1.75
135	30	8.36	±1.80	3.42	±0.885	41.87	±0.77	4683.75	2.61
135	40	19.50	±0.90	5.04	±0.010	42.53	±0.65	8331.67	2.21
165	10	2.02	±0.03	2.04	±0.017	41.27	±1.06	637.59	1.36
165	20	8.71	±0.28	3.62	±0.545	41.53	±0.84	2550.37	1.57
165	30	9.33	±0.33	4.01	±0.020	42.00	±0.85	5724.58	2.07
165	40	23.54	±1.26	7.03	±0.018	43.40	±0.15	10183.15	1.58

±: standard deviation

3.1 Braking distance analysis

The measured braking distance of the V1.0 prototype, as shown in Fig. 4**,** exhibited a clear trend of increasing with both vehicle speed and vehicle mass. The relationship between braking distance and vehicle speed exhibits a quadratic trend, aligning with classical braking physics that ties stopping distance to kinetic energy dissipation. For the 135 kg vehicle, the mean braking distance increased from 1.78 m at 10 km/h to 19.5 m at 40 km/h, while for the 165 kg configuration, the distance at 10 km/h was already higher at 2.02 m, despite missing higher speed data. This underscores the sensitivity of lightweight prototype vehicles to both mass and velocity, confirming studies such as that by Wang *et al.*, who emphasized the influence of inertial force in electric lightweight vehicle dynamics [12].

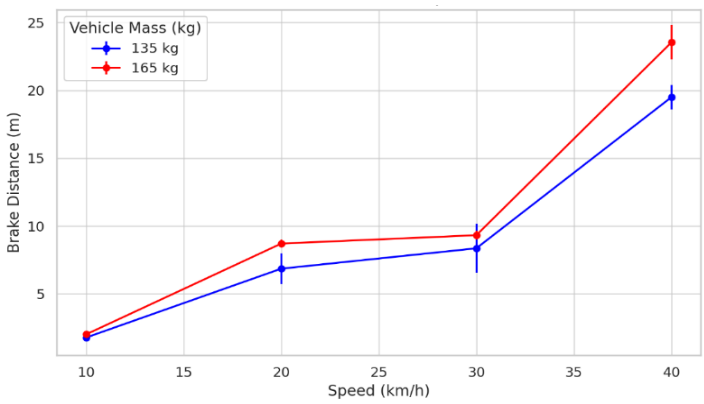

Fig. 4. Measured braking distance

At intermediate speeds of 20 and 30 km/h, the prototype vehicle's braking distances increased substantially, reaching around 6.86 m and 8.36 m for the 135 kg setup, and 8.71 m and 9.33 m for the 165 kg setup, respectively. These values demonstrate how relatively small speed increases can dramatically impact the distance needed to safely stop, particularly when combined with a heavier payload. The difference between the two vehicle masses became more pronounced at these mid-range speeds, reflecting how even modest weight variations can significantly change stopping characteristics [13]. Additionally, Zellner and Weir [3] noted that moderate changes in rear braking or vehicle loading led to different lateral accelerations and stopping behavior, especially under mid-range conditions. This reinforces the point that vehicle mass differences, even if modest, can amplify stopping disparities as speed increases. This highlights the critical importance of accounting for loading conditions when designing braking systems for lightweight prototypes.

The steep rise in stopping distance, especially between 30 and 40 km/h, illustrates that vehicle control and braking system calibration have become increasingly critical at moderate urban speeds. The increased momentum at higher speeds exponentially amplifies the demand on the braking system. Moreover, the standard deviation increases notably with speed, e.g., from 0.13 m at 10 km/h to 1.79 m at 30 km/h, highlighting variability due to possible minor inconsistencies in surface friction, brake pad adhesion, or driver input.

Moreover, these results demonstrate that even at a relatively moderate urban driving speed, a lightweight prototype vehicle can require an unexpectedly long stopping distance, emphasizing the need for proactive safety margins in route design and operational planning [9], [12], [14].

3.2 Braking time analysis

Braking time is a critical indicator of how effectively the braking system can decelerate the vehicle after the brakes are applied. In the V1.0 prototype car, as shown in Fig. 5, braking time consistently increased with vehicle speed, as expected from the fundamental relationship between speed and stopping requirements. Braking time results show a consistent increase in speed, as expected from the kinetic energy-velocity relationship. For the 135-kg prototype, braking time rose from 1.63 s at 10 km/h to 5.04 s at 40 km/h. Interestingly, braking times at 20 and 30 km/h displayed diminishing gains (3.22 s and 3.42 s, respectively), suggesting a possibly nonlinear deceleration trend due to early brake saturation or reduced driver modulation at mid-range speeds. For the 165 kg vehicle traveling at 10 km/h, the braking time was 2.04 s, longer than that of its lighter counterpart at the same speed, confirming that mass increases the time required to stop due to increased inertia. Braking time is fundamentally affected by the available brake force, which in lightweight vehicles can be limited by compact mechanical and hydraulic components [2], [15].

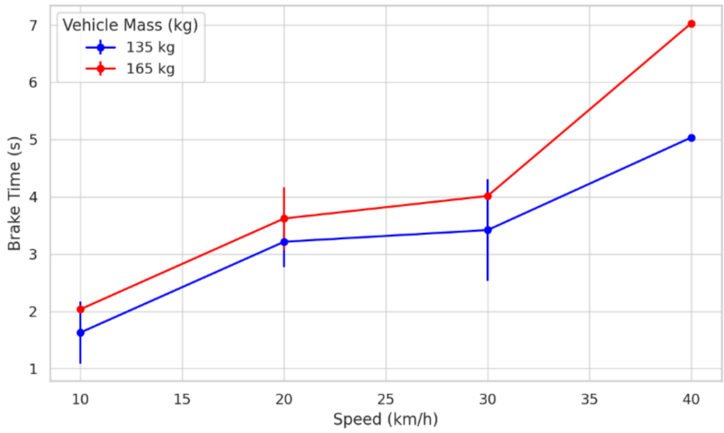

Fig. 5. Measured brake time

The observed performance affirms that while lightweight vehicles possess short stopping ranges, their braking duration can be significantly influenced by payload and velocity. In prototype and urban micromobility applications, brake time needs to be tightly coupled with perception-reaction time modeling to ensure safety under practical deployment scenarios application [2], [15]. The combination of acceptable average times, low standard deviation, and convergence between different vehicle masses at higher speeds suggests that the current brake configuration has been adequately matched to the prototype's size and energy class. However, testing on wet or variable road conditions would be valuable for validating these results under more challenging real-world scenarios, especially given the narrow safety margins of ultra-lightweight prototype platforms.

3.3 Disc pad temperature analysis

Disc pad temperature is a key performance indicator in braking systems, as it directly influences braking effectiveness and the risk of brake fade. Throughout the experimental trials, the V1.0

prototype's disc pad temperature was measured after each braking event to monitor thermal build-up.

As shown in Fig. 6, the disc pad temperature measurements demonstrated a moderate and controlled increase across the tested speed and mass conditions. Temperature behavior across trials reveals minimal thermal stress under single-event braking. The mean disc temperature for the 135-kg vehicle rose modestly from 41.1 °C at 10 km/h to 42.5 °C at 40 km/h, a trend mirrored by standard deviations below 1.15 °C in all conditions. This performance is considered thermally stable and indicates that for short braking distances, the thermal energy conversion through friction is well managed within material tolerances. For the 165 kg configuration at 10 km/h, the temperature remained stable at 41.3 °C, reinforcing the consistency across weight classes at lower kinetic loads.

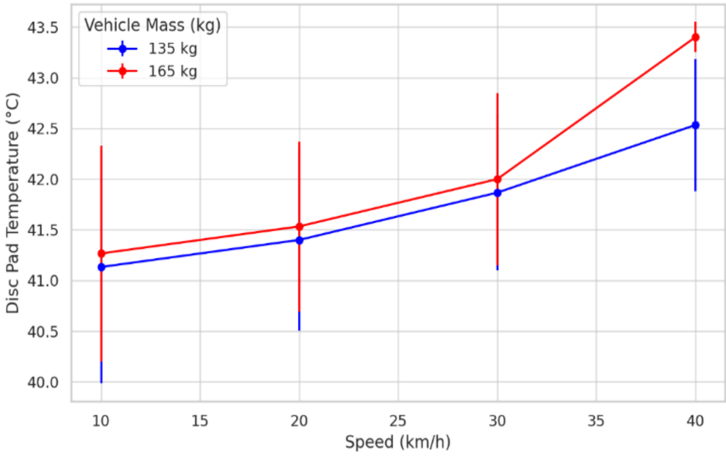

Fig. 6. Disc pad temperature

Recent research by Wang et al. on brake fade dynamics in light electric vehicles supports the view that temperature becomes a concern only during repeated or prolonged braking sequences [16]. Thus, while current thermal behavior is stable, endurance or descent testing may be necessary before certifying this system for repeated braking cycles or competitive scenarios with tight recovery phases. The results affirm the suitability of the current brake pad compound and rotor design for single-stop events under controlled flat surface conditions. However, future designs may benefit from incorporating ventilated discs or regenerative braking hybridization to extend thermal range in extended use cases.

The heatmap analysis of disc pad temperature, as shown in Fig. 7**Error! Reference source not found.** across different speeds and vehicle masses revealed a uniform thermal distribution pattern, with slightly elevated temperatures at higher speeds. This visualization supports the numerical data and confirms that both mass and velocity affect thermal load, but not to a level that compromises safety in single-event braking. The consistent thermal profile (°C) shown in the heatmap reinforces the thermal efficiency of the braking system and its suitability for short-distance, energy-efficient prototypes.

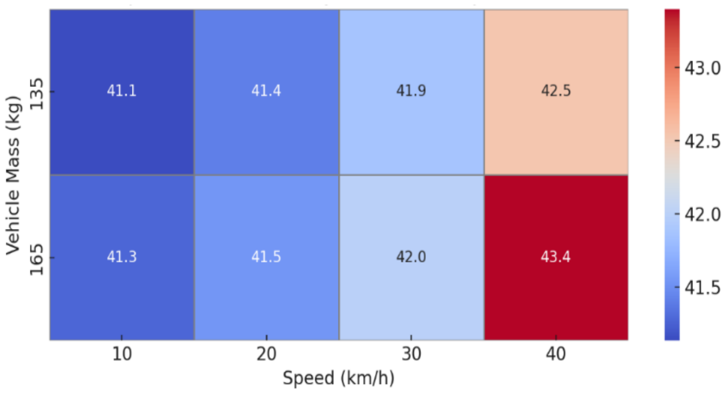

Fig. 7. Heatmap analysis of disc pad temperature

One important observation is that the absolute disc pad temperatures remained well within safe operating thresholds. In conventional vehicle braking systems, disc pads can operate safely at up to 200–300 °C, depending on the material [17], [18], [19]. Therefore, the 43.4 °C maximum observed in this prototype confirms that thermal saturation is not a limiting factor under these test conditions. This is encouraging for prototype competitions, where lightweight braking systems must perform reliably but are rarely stressed to the extremes of heavy-duty passenger or commercial vehicles.

The moderate and repeatable temperature data indicate that the V1.0 prototype's brake system is thermally robust within the tested range. This stability means the braking system is unlikely to suffer from fade or excessive wear under typical prototype usage [20]. However, if the vehicle were to operate at higher sustained speeds or steeper downhill grades, further studies could investigate whether additional cooling or advanced pad materials might be necessary to maintain consistent braking performance over longer duty cycles [17].

3.4 Kinetic energy analysis

The kinetic energy profile, derived from classical mechanics in Eq. (1), emphasizes the exponential growth in energy with speed. As shown in Fig. 8, the 135 kg prototype's kinetic energy rose from ~522 J at 10 km/h to ~8332 J at 40 km/h, indicating a 16x increase with only a 4x increase in speed. For the 165 kg vehicle, the energy at 10 km/h was ~638 J, about 22% higher than the lighter configuration. These findings demonstrate how slight increases in mass or velocity can drastically shift energy demand, reaffirming the nonlinear complexity of vehicle braking control as highlighted by Luo *et al.* [21].

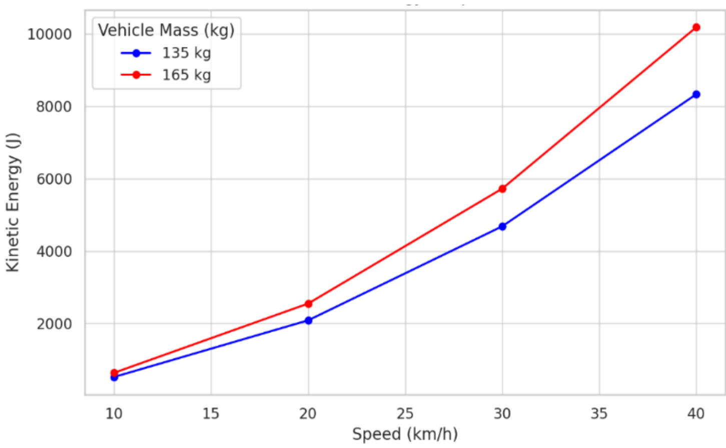

Fig. 8. Kinetic energy as vehicle speed rises

Because braking systems must convert this kinetic energy to thermal and mechanical dissipation, the data corroborate the increasing braking distances and times with higher energy states. These results call for simulation-led brake system calibration during design to ensure optimal performance across speed profiles. Such kinetic energy analysis also underlines why vehicle payload management, route planning, and dynamic weight compensation are increasingly important for safe prototype vehicle operations in dynamic environments.

3.5 Estimated decelerated

Estimated deceleration values, calculated with Eq. (2) as average speed over brake time, highlight how braking effectiveness evolves with conditions. As shown in Fig. 9, for the 135 kg vehicle, deceleration increases from ~1.89 m/s² at 10 km/h to a peak of ~2.61 m/s² at 30 km/h before slightly reducing at 40 km/h (~2.21 m/s²), potentially due to mechanical brake limits or slight tire slip. For the 165 kg vehicle, the deceleration at 10 km/h was lower at ~1.36 m/s², as expected with added mass. It reveals that as speed increases, average deceleration tends to decrease, especially for heavier Vehicles. This inverse relationship suggests that the braking system requires a longer time to reduce the vehicle's momentum at higher speeds. The lower deceleration values in the 165 kg configuration confirm that additional mass reduces braking effectiveness, emphasizing the need for appropriately sized brake components for varying load scenarios [21], [22].

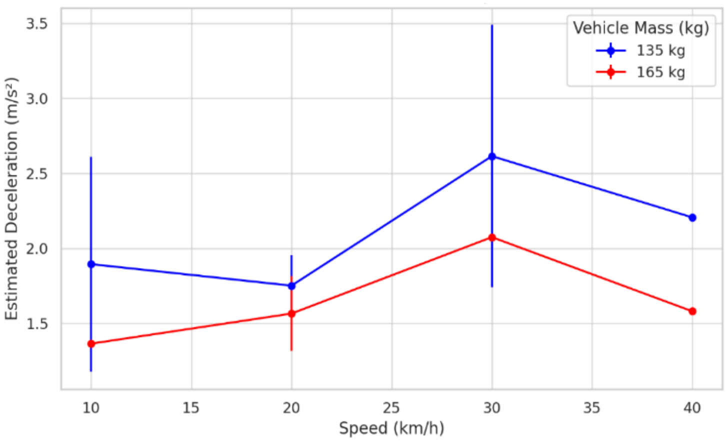

Fig. 9. Estimated deceleration

This pattern shows that while speed and mass both affect kinetic energy, deceleration can vary due to friction limits, brake hardware capabilities, and surface adhesion. Such behavior supports recent conclusions by Jamil et al. that braking response in lightweight electric vehicles must account for non-linear brake efficiency curves, especially under variable loading [23].

The increasing trend followed by a rapid decline may warrant further exploration into the feasibility of Anti-Lock Brake System (ABS) or adaptive brake distribution algorithms in such platforms. These findings underscore the importance of speed-awareness in real-time brake actuation systems for prototype and experimental vehicles. Although there were no signs of thermal overload (as brake pad temperatures remained moderate), the decreasing deceleration trend at higher speeds points to a potential performance ceiling under more demanding operating conditions. Such limitations must be addressed through brake system enhancements, such as increased rotor size or improved material properties [21], [22].

4 Conclusions

This study demonstrates that both vehicle speed and mass significantly influence the braking performance of a low-mass prototype vehicle. Higher speeds and heavier loads increased braking distance and braking time, while disc pad temperatures remained within safe operating limits. These results provide critical insights for optimizing braking system design and ensuring operational safety in lightweight, energy-efficient vehicles. The main results are as follows:

1. At 30 → 40 km/h:

For 135 kg: braking distance rose by 11.14 m (+133%), braking time by 1.92 s (+47%), disc pad temperature by 0.66 °C (+1.5%). Meanwhile, for 165 kg: braking distance rose by 14.21 m (+152%), braking time by 3.02 s (+75%), disc pad temperature by 1.40 °C (+3.3%).

1. Across 10 → 40 km/h (135 kg):

Braking distance increased from 1.78 m to 19.5 m (+995%), and braking time increased from 1.63 s to 5.04 s (+209%).

1. At 30 km/h, adding 30 kg mass increased braking distance by 0.97 m (+11.6%) and braking time by 0.59 s (+17.3%).
2. Disc pad temperatures rose slightly from 41.1 °C to 42.5 °C (increased 3.4%), staying within safe limits.

These results provide a quantitative basis for optimizing braking systems in lightweight, energy-efficient vehicles. They emphasize the importance of managing load conditions, calibrating brake systems for various speeds, and accounting for weight transfer effects in design.

References

[1] T. D. Gillespie, *Fundamentals of Vehicle Dynamics*. Warrendale, PA: SAE International, 1992. doi: 10.4271/R-114.

[2] J. T. Bray, G. R. Walker, A. G. Simpson, M. C. Greaves, and N. A. B.D.Guymer, "Brake system performance requirements of a lightweight electric/hybrid rear wheel drive vehicle," International Journal of Vehicle Autonomous Systems, vol. 1, no. 3/4, p. 436, 2003, doi: 10.1504/IJVAS.2003.004382.

[3] J. W. Zellner and D. H. Weir, "Motorcycle Braking Test Procedures and Performance," *SAE Transactions*, vol. 89, pp. 966–973, 1980, [Online]. Available: http://www.jstor.org/stable/44632469

[4] P. Wulf, *Brakes, Brake Control and Driver Assistance Systems*. Wiesbaden: Springer Fachmedien Wiesbaden, 2014. doi: 10.1007/978-3-658-03978-3.

[5] J. Y. Wong, *theory of ground vehicles*, 5th ed. John Wiley & Sons, 2022.

[6] Y. Chen, Z. Zhang, C. Neighborgall, and M. Ahmadian, "When is it too late to brake?," *Vehicle System Dynamics*, vol. 61, no. 11, pp. 2888–2911, Nov. 2023, doi: 10.1080/00423114.2022.2144386.

[7] Y.-S. Chen, S.-C. Chiu, and S.-S. Hsiau, "Safe Technology with a Novel Rear Collision Avoidance System of Vehicles," *International Journal of Automotive Technology*, vol. 20, no. 4, pp. 693–699, Aug. 2019, doi: 10.1007/s12239-019-0065-0.

[8] J. Broniszewski and J. Piechna, "A fully coupled analysis of unsteady aerodynamics impact on vehicle dynamics during braking," *Engineering Applications of Computational Fluid Mechanics*, vol. 13, no. 1, pp. 623–641, Jan. 2019, doi: 10.1080/19942060.2019.1616326.

[9] D. Berjoza, I. Dukulis, V. Pirs, and I. Jurgena, "Testing Automobile Braking Parameters by Varying The Load Weight," 2019. Accessed: Aug. 08, 2025. [Online]. Available: https://proceedings.tae-conference.cz/2019/

[10] D. B. Antanaitis, "A Study of Mass Drivers in the Brake System," *SAE International Journal of Passenger Cars - Mechanical Systems*, vol. 7, no. 4, pp. 2014-01–2506, Sep. 2014, doi: 10.4271/2014-01-2506.

[11] Q. Liu, C. Zhang, T. J. Gordon, and J. Wang, "Dynamics and control of articulated passenger vehicles on roads," *Vehicle System Dynamics*, vol. 63, no. 7, pp. 1395–1457, Jul. 2025, doi: 10.1080/00423114.2025.2507405.

[12] R. Wang, Y. Jiang, R. Ding, W. Liu, X. Meng, and Z. Sun, "Design and experimental verification of self-powered electromagnetic vibration suppression and absorption system for in-wheel motor electric vehicles," *Journal of Vibration and Control*, vol. 28, no. 19–20, pp. 2544–2555, Oct. 2022, doi: 10.1177/10775463211014419.

[13] E. G. Sayed, M. M. M. Makrahy, M. R. Sharkawy, and K. A. A. Gawwad, "Effect of Normal Force, Sliding Speed, Temperature, and Al_2O_3 Addition on Wedge and Conventional Disc Brake Performance," *Indonesian Journal of Innovation and Applied Sciences (IJIAS)*, vol. 5, no. 2, pp. 182–192, Jun. 2025, doi: 10.47540/ijias.v5i2.1996.

[14] Y. Zeng, H. Ding, R.-H. Du, and L.-Q. Chen, "A suspension system with quasi-zero stiffness characteristics and inerter nonlinear energy sink," *Journal of Vibration and Control*, vol. 28, no. 1–2, pp. 143–158, Jan. 2022, doi: 10.1177/1077546320972904.

[15] P. G. Anselma, S. P. Patil, and G. Belingardi, "Rapid Optimal Design of a Light Vehicle Hydraulic Brake System," Apr. 2019. doi: 10.4271/2019-01-0831.

[16] X. Wang and J. Zuo, "Thermal Analysis of Brake Discs under the Effect of Dynamic Forces," *Tribology Transactions*, vol.

68, no. 3, pp. 489–497, May 2025, doi: 10.1080/10402004.2025.2482612.

[17] Q. Zhang *et al.*, “Impact of initial braking temperature on thermal-induced brake fade during long-downhill operations,” *Eng Fail Anal*, vol. 167, p. 109077, Jan. 2025, doi: 10.1016/J.ENGFAILANAL.2024.109077.

[18] M. Kchaou, A. Sellami, J. Fajoui, R. Kus, R. Elleuch, and F. Jacquemin, “Tribological performance characterization of brake friction materials: What test? What coefficient of friction?,” *Proceedings of the Institution of Mechanical Engineers, Part J: Journal of Engineering Tribology*, vol. 233, no. 1, pp. 214–226, Jan. 2019, doi: 10.1177/1350650118764167.

[19] S. Vivek, L. S. Jayakumari, S. Stephen Bernard, G. Suresh, M. J. Ahmed, and S. Arulmurugan, “Tribological and mechanical properties of biobased reinforcement in a friction composite material,” *Revista Materia*, vol. 25, no. 3, p. 1, 2020, doi: 10.1590/s1517-707620200003.1085.

[20] M. A. Essam, M. M. Faragallah, M. Magdy, and N. M. Abdeltawab, “Effect of sliding velocity, load, and RPM on wear and friction in automotive brake pads,” *Discover Applied Sciences*, vol. 7, no. 5, p. 453, May 2025, doi: 10.1007/s42452-025-06925-2.

[21] T. Luo, N. Luo, J. Yang, and B. Huang, “Parameter Optimization Methods of the Hydraulic Regenerative Braking System Based on the Actual Working Condition,” in *The 8th International Conference on Advances in Construction Machinery and Vehicle Engineering*, S. K. Halgamuge, H. Zhang, D. Zhao, and Y. Bian, Eds., Singapore: Springer Nature Singapore, 2024, pp. 159–173.

[22] Z. Chen, R. Xiong, X. Cai, Z. Wang, and R. Yang, “Regenerative Braking Control Strategy for Distributed Drive Electric Vehicles Based on Slope and Mass Co-Estimation,” *IEEE Transactions on Intelligent Transportation Systems*, vol. 24, no. 12, pp. 14610–14619, 2023, doi: 10.1109/TITS.2023.3299313.

[23] H. Jamil, S. S. A. Naqvi, N. Iqbal, and M. A. Khan, “Analysis on the Driving and Braking Control Logic Algorithm for Mobility Energy Efficiency in Electric Vehicle,” *Smart Grids and Sustainable Energy*, vol. 9, no. 1, p. 12, Feb. 2024, doi: 10.1007/s40866-023-00190-1.